Title

Flexible all-organic nanocomposite films interlayered with in situ synthesized covalent organic frameworks for electrostatic energy storage

Authors

Li, He

Xie, Zongliang

Yang, Chongqing

et al.

Publication Date

2023-08-01

DOI

10.1016/j.nanoen.2023.108544

Flexible all-organic nanocomposite films interlayered with *in situ* synthesized covalent organic frameworks for electrostatic energy storage

*He Li[a,b,1], Zongliang Xie[c,1], Chongqing Yang[b], Junpyo Kwon[a,d], Antoine Lainé[a], Chaochao Dun[b], Alexander V. Galoustian[b,e], Xinle Li[b,f], Peng Liu[c], Jeffrey J. Urban[b], Zongren Peng[c], Miquel Salmeron[a,g], Robert O. Ritchie[a,d,g], Ting Xu[a,g,h], and Yi Liu[a,b,]**

[a] Materials Sciences Division, Lawrence Berkeley National Laboratory, Berkeley, CA 94720, USA

[b] The Molecular Foundry, Lawrence Berkeley National Laboratory, Berkeley, CA 94720, USA

[c] State Key Laboratory of Electrical Insulation and Power Equipment, School of Electrical Engineering, Xi'an Jiaotong University, Xi'an, Shaanxi 710049, China

[d] Department of Mechanical Engineering, University of California, Berkeley, Berkeley, CA 94720, USA

[e] Department of Chemical and Biomolecular Engineering, University of California, Berkeley, CA 94720, USA

[f] Department of Chemistry, Clark Atlanta University, Atlanta, GA 30314, USA

[g] Department of Materials Science and Engineering, University of California, Berkeley, CA 94720, USA

[h] Department of Chemistry, University of California, Berkeley, CA 94720, USA

*Corresponding author
E-mail address: yliu@lbl.gov
[1] These authors contributed equally to this work.

ABSTRACT:

Poly(vinylidene fluoride)-based terpolymers, known for having the largest dielectric constant among the existing dielectric polymers, are attractive materials for electrostatic film capacitors used in lightweight electrification systems. However, their potential for such applications is limited by low electrical and mechanical strengths. To address such limitations, we introduced rigid covalent organic framework (COF) nanospheres into the thin films of soft terpolymers via *in situ* synthesis and a facile layer-by-layer solution casting method, whereby multilayer films containing two polymer outer layers and a COF-containing middle layer were readily obtained. The resultant all-organic thin films exhibit simultaneously high dielectric constant, enhanced breakdown strength, superior energy density (~25 J cm^{-3}) at efficiencies over 80%, along with improved mechanical self-supporting capability and excellent mechanical flexibility. This work demonstrates the unprecedented use of COF for electrostatic energy storage, uncovering its potential for flexible electronic applications operating under high electric fields.

KEYWORDS: covalent organic framework; energy storage; in situ synthesis; layered structure; nanocomposite; thin film fabrication

1. Introduction

With the rapid advancements in science and technology, the demand for high-performing energy storage devices has been continuously increasing. Dielectric capacitors (i.e., electrostatic capacitors), which store charges electrostatically, have the fastest discharging rate compared to electrochemical supercapacitors and batteries.[1-4] In particular, polymer-based electrostatic film capacitors exhibit several intrinsic merits, including greater processability, flexibility, lightweight and voltage tolerance capability with respect to inorganic dielectric ceramics,[5-14] making them an ideal choice for microelectronics and power systems. Because polymer-based film capacitors constitute over 25% of the volume and weight of electric power systems, as exemplified in the power inverter of hybrid electric vehicles,[7] enhancement in energy density of film capacitors would be conducive to reducing the volume, weight, and cost of electrified systems such as electric vehicles and aircrafts. As the charged energy density of a dielectric material is positively related to its dielectric constant (k) and dielectric breakdown strength (E_b), it is imperative to develop polymer dielectrics with concurrently large k and E_b values to achieve high energy densities.

Poly(vinylidene fluoride) (PVDF) and its multipolymers with relatively high k (i.e., $\geq$ 10 at 1 kHz) have been regarded as the most promising polymer candidates for high-energy-density electrostatic film capacitors.[15-20] A unique class of PVDF-based polymers is the terpolymers represented by poly(vinylidene fluoride-*ter*-trifluoroethylene-*ter*-chlorofluoroethylene) P(VDF-TrFE-CFE) (abbreviated as PVTC hereafter), which possess the largest k values (i.e., ~40–50 at 1 kHz) among the known dielectric polymers.[21-23] However, chlorofluoroethylene moieties act as defective units along the polymer backbone, unfortunately degrading the terpolymers' mechanical strength. The Young's modulus (Y) of PVTC is only around 100 MPa, relative to ~700 MPa of pure PVDF.[24] Since the electromechanical mechanism dictates the dielectric breakdown behavior of

soft materials (e.g., dielectric polymers),[25,26] the undesirable mechanical modulus of PVTC leads to an inferior E_b (i.e., ≤ 400 MV m^{-1}) when compared with those of PVDF and its copolymers. Furthermore, PVTC is too soft to be fabricated into free-standing, wrinkle-free thin films (i.e., <10 μm), which restricts their practical use in roll-to-roll assembled film capacitors.[27] In the past decade, inorganic nanofiller doping[27-32] and organic component blending[33,34] have been adopted to improve the electrical and mechanical strength of PVDF-based terpolymers. For example, Wang and coworkers utilized boron nitride nanosheets to enhance E_b and Y of PVTC, realizing a high discharged energy density (U_d) of 20.3 J cm^{-3} at 650 MV m^{-1} in the organic/inorganic nanocomposite film;[27] Nan and coworkers mixed PVDF with PVTC to yield an all-organic polymeric film with a high U_d of 19.6 J m^{-3} at 640 MV m^{-1}.[34] However, the organic/inorganic interfacial compatibility remains a challenge for the former approach,[3,9] while the latter strategy demonstrates moderate success since the k value of terpolymers drops markedly once blended with other low-k polymers.[33] To date, even if the PVTC holds the distinctive feature of high-k, its potential for electrostatic film capacitors is still far from fully explored and demands innovative solutions.

In the quest for ideal organic fillers for all-organic PVTC-based composite films, two-dimensional (2D) covalent organic frameworks (COFs) have emerged as attractive candidates despite the dearth of related dielectric studies.[35-37] Different from the conventional linear polymers, which are typically flexible and amorphous,[7] 2D COFs are highly crosslinked yet structured polymers boasting greater mechanical robustness and higher crystallinity due to the high degree of crosslinking and the rigidity of the chemical constituents.[38-40] While the mechanical perspective of 2D COFs as organic fillers is quite attempting, practical hurdles arise from the severely diminished processibility of COF materials as a result of increased rigidity and

crystallinity, limiting their direct incorporation into large-area, high-quality thin films compatible with device fabrication and characterization for practical applications.[41-43] In order to take advantage of COF's superior mechanical strength[40] while resolving the processibility issue, we envision that nanostructured COFs, instead of continuous COF films, could be used to prepare composite thin films by incorporating them in the matrix of dielectric polymers such as PVTC. The all-organic nature of COF nanostructures and PVTC will engender the desired compatibility, circumventing issues caused by defective organic/inorganic interfaces that are common in conventional polymer nanocomposites.[3,9] Recent synthetic advances have enabled facile access to COFs with tailored nanostructures through the control of the nucleation and growth of COF crystallites.[44] For example, spherical imine-linked COF nanoparticles could be readily obtained from solution-based condensation reactions between multivalent aldehyde and amine precursors.[45] Thus, how to integrate COF nanoparticles into free-standing composite films is the key to unlocking the full potential of COFs for flexible electronic applications.[43]

In this work, we tackled the processing challenges and devise a feasible approach to achieving flexible composite films by incorporating a layer of uniform COF nanospheres within two layers of PVTC polymer. The sandwich-structured polymer/COF hybrid films were prepared through a facile layer-by-layer solution casting method, in which the middle layer of imine-linked COF nanospheres was formed *in situ* at room temperature within minutes. The synergistic combination of a layer containing rigid COF nanoparticles and two layers of soft terpolymer incurs excellent mechanical flexibility while retaining the high-Y characteristic of the COFs, yielding sandwich films with significantly improved mechanical self-supporting capability. To the best of our knowledge, this represents the first example of all-organic COF/polymer composites for electrostatic energy storage applications. The resultant capacitor devices based on the optimized hierarchical

composite thin films display simultaneously large k and E_b values, endowing a high U_d of ~25 J cm^{-3} coupled with a high energy efficiency of >80%. This U_d value is nearly five-fold and three-fold higher than those of the industrial benchmark biaxially-oriented polypropylene (BOPP) film capacitor and the native PVTC film, respectively. Furthermore, successive charging/discharging test and mechanical bending test validate that the developed hybrid films can operate reliably under high electric field conditions.

2. Results and discussion

2.1 Materials preparation and structural characterization

It has been predicted theoretically and confirmed experimentally that polymer composite films with optimized layered structures would yield improved dielectric and energy storage performance relative to single-layer films.[46-49] In particular, the symmetrical sandwich structure design for dielectric polymer composites has been demonstrated as a viable approach that can facilely modulate multiple dielectric parameters by tailoring the chemical structures, interfaces and compositions of the contiguous layers.[50-54] Since the E_b of polymer dielectrics is highly dependent on Y, a larger Y typically gives rise to a higher E_b in most polymer dielectrics, especially for the soft PVDF-based polymers and nanocomposites.[26,27,55] Moreover, it is found that the intercalation of an inorganic layer between two polymeric layers can repulse the extension of the electrical breakdown pathway across polymer dielectrics.[56-58] On the basis of the above considerations, we surmise that by leveraging the advantages of the constituent layers, i.e., high k of the polymer layers and high Y of the COF layer, simultaneous enhancement of electrical and mechanical strengths can be achieved in the PVTC-based films sandwiched with a COF-containing middle layer.

The sandwich-structured all-organic polymer nanocomposite films were prepared via a layer-by-layer drop casting method, as depicted in **Scheme 1**. The thickness of three-layer films was controlled to be approximately the same as that of the single-layer PVTC films, and the ratio of the thickness for each layer was fixed as approximately 1:1:1.[59] 2,5-dimethoxyterephthalaldehyde (DMTA) and 1,3,5-tri-(4-aminophenyl)benzene (TAPB) were selected as precursors for the synthesis of middle COF layer, given that excellent electrical insulation strength has been proven in this imine-linked COF film.[35] In addition, as solvent is known to play a crucial role in

determining the crystallinity and morphology of COFs,[44,45] we studied the effects of different solvents (i.e., acetonitrile (MeCN), methanol and *o*-dichlorobenzene) on the growth of COF nanoparticles. As summarized in Figs. S1 and S2, MeCN stands out as the good solvent since the thus-synthesized COF nanoparticles have the most well-defined morphology, which appear as monodispersed nanospheres with an average diameter of 200–300 nm, together with the most pronounced crystallinity, as evidenced by powder X-ray diffraction (XRD) analysis. Under the optimized condition involving MeCN as the solvent and acetic acid as the catalyst,[45] a high-quality layer of imine-linked COF nanospheres was formed via a rapid synthesis under ambient condition. According to the scanning electron microscopic (SEM) images, however, it was observed that even though the spherical COF nanoparticles were densely packed, microscopic defects were persistent throughout the layer due to the imperfect packing (**Fig. 1A**), which was undesirable for electrical insulation, especially under high electric fields (see the discussion below).

To improve the packing within the sandwich layer, a new protocol was developed by integrating the PVTC additive into the COF precursor solution for the *in situ* COF synthesis. Thanks to the excellent solubility of PVTC in MeCN, a homogeneous solution could be obtained and subsequently cast to produce sandwich films containing an intercalated PVTC/COF middle layer. Different weight fractions of PVTC additive were employed in the reaction mixtures for the fabrication of middle layers. The resulting sandwich films with various PVTC compositions in the middle layer are denoted as **S-*x***, where *x* represents the approximate weight fraction of the PVTC additive. For instance, **S-0** represents the polymer film with a pure COF middle layer, while **S-20** represents the polymer film with a PVTC/COF middle layer in a weight ratio of about 20% polymer and 80% COF precursors. When the weight ratios of polymer additive were less than 60%, a continuous middle layer was formed where PVTC terpolymer and COF particles co-existed with

high compatibility. The intercalated COF layers displayed well-retained crystallinity and spherical morphology of the COF particles, as supported by SEM and XRD studies. The SEM images of a cross-section of **S-20** indicated that the PVTC additive effectively filled the void space among COF particles, in sharp contrast to **S-0** where gaps were clearly visible in the pure COF layer (**Figs. 1B** and S3). XRD spectra revealed the characteristic diffraction peaks of COFs in the presence of various fractions of polymer additives (**Fig. 1C**). Interestingly, those diffraction peaks displayed small but consistent shift to higher 2θ angles upon the increase of polymer additive fraction. For instance, the [100] peak shifted from 2θ of 2.76° for pure COF to 2.78°, 2.80° and 2.82° for *in situ* synthesized COFs with 20, 40 and 60 wt% PVTC additives, respectively. After washing away PVTC binder from the polymer/COF composites using MeCN, the characteristic XRD peak positions of all the COF samples were restored to those identical to the pure COF (**Fig. 1D**), suggesting that the lattice distortions in **S-*x*** (x = 20, 40 and 60) were due to non-covalent and reversible interactions between the COF and PVTC terpolymer. Further N_2 adsorption analysis reveals that the Brunauer–Emmett–Teller (BET) surface areas of the COF-containing layers in **S-0** and **S-20** were comparable after MeCN wash (757 *vs.* 587 $m^2\ g^{-1}$), and both samples have a narrow pore width distribution at ~3.3 nm, suggesting that PVTC binder did not impede the formation of nanometer-sized pores within the COF particles (Fig. S4). Fourier-transform infrared (FTIR) spectroscopy and X-ray photoelectron spectroscopy (XPS) results reaffirmed that there was no covalent bond formation at the COF-terpolymer interfaces during the *in situ* synthesis (Figs. S5 and S6). It is worth noting that no additional solvent treatment step was adopted to remove potential residual monomers or side products embedded within the COF nanospheres for the sake of preserving the high quality of composite films, which is more important for electronic device fabrication.

2.2 Dielectric breakdown behavior and mechanism analysis

Dielectric breakdown strength (E_b) of a series of sandwich-structured PVTC/COF films and native PVTC film was analyzed based on a two-parameter Weibull statistic model that can be described as $P(E) = 1–\exp(–(E/\alpha)^{\beta})$, where $P(E)$ is the cumulative probability of dielectric breakdown failure, E is the experimental dielectric breakdown field, α is the scale parameter, also known as Weibull breakdown strength (Weibull E_b), which corresponds to a failure probability of 63%, β is the shape parameter that is inversely associated with the dispersion degree of experimental data. The fitting results are plotted as the probability of failure (expressed as $\ln(–\ln(1–P))$ *versus* the natural logarithm of E, as shown in **Fig. 2A**. Correspondingly, **Fig. 2B** and Table S1 summarize the extracted Weibull E_b and β values from Weibull plots. The **S-0** sample, i.e., sandwich film interlayered with an all-COF layer, represents a ~30% increment in Weibull E_b compared to that of single-layer PVTC (i.e., 415 *vs.* 553 MV m^{-1}). However, a severe reduction in β is found from 9.1 of PVTC to 5.3 of the **S-0** film. On the contrary, the incorporation of PVTC/COF composite interlayers increases Weibull E_b and β values of the polymer films simultaneously, which are maximized at 697 MV m^{-1} (for the **S-20** sample) and 16.0 (for the **S-10** sample). These values amount to 68% and 76% enhancements, respectively, compared to the neat PVTC film. Clearly, the utilization of polymer additives for COF interlayer synthesis is beneficial for further improving the film quality and E_b of PVTC, underscoring the importance of polymer filler to annihilate defective void spaces between COF particles for achieving high electrical insulation strength.

To better understand the pronounced improvement in E_b of the sandwich-structured hybrid films, we performed systematic investigations on their mechanical strength and electrical conduction properties, which are two well-recognized main factors that impact E_b of soft matters.[25-27] When an electrostatic film capacitor is charged under an electric field, the coulomb force is induced on the

opposite electrodes, which is then converted into electromechanical stress and can lead to the breakdown across the capacitor film.[25] Therefore, high mechanical strength is desirable for polymer dielectrics, given that the larger Young's modulus (Y) would provide a higher capacity to withstand coulomb force, thereby reducing electromechanical failure. Y of the COFs, obtained from nanoindentation (Fig. S7), is more than an order of magnitude larger than that of the host terpolymer (i.e., ~1.1 GPa *vs.* ~60 MPa). Additionally, tensile tests were employed to assess the Y of the integrated three-layer films (**Figs. 2B** and S8). The Y of films increased remarkably with increasing COF ratio in the interlayer, e.g., from ~95 MPa of native PVTC to ~232 MPa of the **S-20** sample and ~323 MPa of the **S-0** sample. A quantitative analysis of the Y–E_b correlation was carried out based on an electromechanical breakdown model: $E_{em} = 0.606(Y/(k\varepsilon_0))^{1/2}$,[25] where E_{em} is the theoretical electromechanical breakdown field, ε_0 is the permittivity of vacuum, k is the dielectric constant. **Figs. 2D** and S9 display the dielectric spectra of PVTC-based dielectric materials as a function of frequency. At low frequencies, PVTC dipoles have sufficient time to align with the electric field before it changes direction. At high frequencies (10^5–10^6 Hz), characteristic dipole relaxation, known as α_a relaxation, occurs, resulting from the segmental motion of polymer chains[60,61]. This phenomenon is commonly observed in PVDF-based dielectric polymers[16,19,27]. When the frequency domain enters this relaxation range, the dipoles cannot keep up with the frequency to align before the direction of the electric field changes, leading to a drop in k and an associated loss tangent peak, as seen in the dielectric spectra[61]. Additionally, the effective k extracted from electric polarization-electric field (P-E) loops indicates that the k values of these films also vary with the electric field. (Fig. S10) Given the fact that the breakdown event occurred under relatively high electric fields, we utilized the effective k at the electric field near the E_b for theoretical calculations. The E_{em} values of the sandwich films were predicted to follow a

monotonically increasing trend with the increase of COF ratio in the interlayer (Fig. S11), which clearly differed from the trend for experimental Weibull E_b values. The inconsistency between the two suggested that there were additional contributing factors to the breakdown strength other than electromechanical strength, despite that electromechanical breakdown was the primary mechanism responsible for electrical failure in PVDF-based dielectric materials.[27] It is worth noting that the above electromechanical model assumes no free charges across the dielectric when applying an electric field.[25,27] Electrical conduction, nonetheless, should not be underestimated in a dielectric material of practical usage, which would trigger the development of breakdown paths, especially under the stimulus of a high electric field.[7,27] As shown in **Fig. 2E**, the sandwich film **S-0** displayed the poorest electrical resistivity, corroborating with higher leakage current due to the defective packing of COF particles in the middle layer. For the sandwich samples with different compositions, the trend of Weibull E_bs correlated well with the trend of electrical resistivity, both reaching maximum in the **S-20** sample (Fig. S12). The difference in electrical resistivity may account for the discrepancy between the experimental and theoretical breakdown strengths of such sandwich hybrid films.

To study the influence of the spatial distribution of fillers on E_b of the polymer composites, a variety of single-layer PVTC/COF nanocomposite films were fabricated via casting PVTC solutions containing randomly dispersed COF particles (see Supplemental information for details). For comparison purposes, the amounts of COFs employed in the single-layer PVTC/COF composite films were fixed to be the same as those in the corresponding sandwich-structured films, i.e., ~13.3–30 wt% of COFs relative to the total mass of the films. The Weibull statistic results of the single-layer composites were shown in **Fig. 3A**, where the Weibull E_b increased initially upon the introduction of COF nanoparticles and was maximized at 486 MV m^{-1} for the composite with 16.7

wt% COF. Further increase of the COF loading led to a steady decrease in Weibull E_b of the composite films (e.g., 373 MV m^{-1} of the 30 wt% COF-loaded sample). This trend was in agreement with most conventional polymer nanocomposites consisting of inorganic particles,[4,24,27-29,62-65] where an optimized filler concentration was critical to realizing the maximal enhancement in electrical properties. In addition, it was found that the single-layer composites had a much lower optimal concentration compared to the sandwich-structured composites (**Fig. 3B**). At the same COF weight fraction, the hybrid films with a sandwich structure displayed a higher capacity to withstand mechanical failure and electrical leakage, as well as greater dielectric strength and stability (i.e., larger E_b and β values, respectively), compared to those single-layer films containing randomly dispersed COF particles (Figs. S13 and S14, Table S2).

To gain insight into the mechanistic impact of the COF distribution on the breakdown behavior of the polymer composite films, we conducted finite element simulations and statistical predictions on three systems, including neat PVTC, sandwich-structured and randomly dispersed single-layer PVTC/COF composites. The simulation models were built based on images processed from cross-sectional SEM images, which were labeled as **Model i**, **Model ii** and **Model iii**, respectively (see Fig. S15). The simulated electric field and leakage current distributions of these three systems were shown in Fig. S16. The results indicated that the interlayer in **Model ii** could redistribute the electric field and leakage current to prevent the weak phase (i.e., PVTC terpolymer) from bearing excessive electric stimuli. For instance, when applying an electric field of 50 MV m^{-1} on these models, the average field strength and current density of the terpolymer phase were alleviated respectively by 36.6% and 44.2%, i.e., 31.69 MV m^{-1} and 1.12×10^{-7} A cm^{-2} for **Model ii** compared to those of 50 MV m^{-1} and 2×10^{-7} A cm^{-2} for **Model i**. In contrast, the randomly dispersed COF particles in **Model iii** exhibited limited capacity in protecting the terpolymer phase from the applied high

electric field. Further dielectric breakdown simulations were carried out based on statistical predictions using a modified dielectric breakdown model (DBM, see Simulation Section and Figs. S17 and S18). As summarized in Fig. S19, it was clear that the growth of the breakdown path distorted the local electric field distribution at the end of a branch. Relative to COF-free **Model i**, the existence of COF interlayer with high *Y* effectively strived against electrical stress and hindered the propagation of electrical breakdown path (**Model ii**), while the random distribution of COF particles in **Model iii** promoted the scattering of discharge channels but played a limited role in suppressing breakdown path extension. Consequently, the breakdown channel in **Model ii** was better restrained relative to those in **Models i** and **iii**, under the same simulation condition (**Figs. 3C** to **3E**).

2.3 Energy storage performance and reliability assessment

The electrostatic energy storage performance of the sandwich PVTC/COF composite films, along with the control polymer film, were thoroughly assessed (Figs. S20 and S21). **Figs. 4A** and **4B** depicted the unipolar *P-E* loops of PVTC polymer and the sandwich-structured PVTC/COF composite (**S-20)** at their respective highest withstanding electric fields, where significantly improved electric field tolerance and electric polarization were observed in the loop of the *in situ* synthesized sandwich film relative to neat terpolymer. As compared in **Fig. 4C**, the sandwich film **S-20** displayed the largest U_d of 24.6 J cm^{-3} along with a charge-discharge efficiency (η) of 80.7% at 700 MV m^{-1}, far exceeding those of the native PVTC film (i.e., 9.2 J cm^{-3} and 68.0% at 400 MV m^{-1}). The maximum U_d of **S-20** was also about five times higher than that of the commercial benchmark BOPP dielectric film under the same test condition (Fig. S22). The favorable energy storage capacity was attributed to the concomitant enhancements of electrical resistivity, Y, and E_b, as demonstrated in **Fig. 4D**. The k values of the sandwich PVTC/COF composites, on the other hand, were lower than that of the neat terpolymer (36.6 *vs.* 46.9, at 1 kHz), primarily because the loaded COF has an inherently lower k due to the weaker dipolar polarization and non-ferroelectric feature compared to the PVTC matrix (Fig. S23).[19,27] Nonetheless, the moderately reduced k value did not compromise the overall energy storage properties of the hybrid composite due to the large gain in electrical resistivity, Y, and E_b. Apart from U_d, η is another essential metrics for evaluating the practical energy storage performance of dielectric materials. High η is desirable to minimize Joule heat from energy loss and to increase the reliability and lifespan of electrostatic capacitors while a low η will overwhelm any other benefits gained by enhanced k, E_b and U_d. However, the majority of existing PVDF terpolymer-based dielectrics can only reach mediocre η values, typically around 50–70% at the materials' withstanding electric fields. As shown in **Fig. 4E**,

the **S-20** film exhibits superior U_d value when compared to the reported PVDF terpolymer-based dielectric thin films at efficiencies above 80%.[27-33, 66-70] Fig. S24 also listed the U_d and η of high-energy-density dielectric thin films based on terpolymers, among which the **S-20** film shows the remarkable balance between η (>80%) and the maximal U_d (~25 J cm^{-3}). The enhancement in energy storage performance induced by COF interlayers can be rationalized as the following: the presence of COF restrains early polarization saturation of ferroelectric polymer (see Fig. S25), which allows the hybrid composite to retain relatively large efficient k values (see Fig. S10) and to store more electrical energy under high electric fields.[71] As shown in Fig. S26, the samples **S-60**, **S-40**, and **S-20** showed lower maximum polarization (P_m) than PVTC at low field regions (<300 MV m^{-1}), e.g., at 100 MV m^{-1}. The P_m of PVTC, **S-60**, **S-40** and **S-20** decreased monotonously from 4.38 to 4.17, 3.74 and 3.21 μC m^{-2}, primarily due to the COF's low-k feature. However, with an increase in electric field, these sandwich-structured COF-containing samples exhibited higher P_m than PVTC, consistent with the trend observed in the field-dependent effective k derived from the P-E loops. Notably, the maximum P_m was 11.90 μC m^{-2} at 700 MV m^{-1} for **S-20** and 8.96 μC m^{-2} at 400 MV m^{-1} for neat PVTC, indicating markedly improved energy storage performance. The lower P_m of **S-0** compared to PVTC across the investigated field range may reflect the nonideal packing of COF nanospheres within the middle layer of **S-0**, which limited electric polarization under applied electric fields. Moreover, the sandwich-structured hybrid films exhibited vastly reduced energy loss, as demonstrated by the suppressed remnant polarization (P_r) in Fig. S27, indicative of the inherently low loss of the COF material and its contribution to enhanced energy efficiencies.

For pulsed applications, power density is another critical metrics in addition to U_d and η. We performed fast discharge tests to evaluate the power density of the *in situ* synthesized sandwich PVTC/COF composite film, as shown in Fig. S28. At an applied electric field of 200 MV m^{-1}, which

is the working field of electrostatic capacitors in common power systems such as hybrid electric vehicles,[5] the sandwich hybrid film **S-20** displayed a power density nearly eight-fold of that of BOPP (110.57 *vs.* 13.92 MW L^{-3}). **Fig. 4F** showed the cyclic charging/discharging measurement result of the sandwich film under the same electric field of 200 MV m^{-1}, where almost no sign of deterioration in energy storage performance was observed over 50,000 continuous charge-discharge cycles. The initial increase in η and decrease in U_d were attributed to the gradual alignment of ferroelectric domains with the applied electric field.[71,72] When most of the ferroelectric dipoles were aligned with the field (after dozens of charging/discharging cycles), the data variations in U_d and η were smaller than 1.04% and 2.41%, respectively. The values are comparable to those of the benchmark BOPP dielectric film under the same test condition (Fig. S29).

Mechanical bending tests were further carried out to evaluate the mechanical flexibility and reliability of the sandwich PVTC/COF hybrid film, properties that are essential for future wound capacitor cell fabrication. It is noteworthy that although free-standing thin film (thickness ~9 μm) of native PVTC can be prepared under careful lab-scale operation, bending without causing wrinkles is challenging because the polymer is too soft to support itself efficaciously. In contrast, the intercalated COF-containing layer functions as a robust scaffold in the sandwich film, which significantly enhances the mechanical self-supporting capability of PVTC polymer, as shown in Fig. S30. Moreover, the inclusion of terpolymer additives creates a flexible buffer among neighboring COF particles, ensuring the integrity of an intact interlayer in the sandwich-structured hybrid film when subjected to mechanical bending stress. The mechanical endurance was validated by the results shown in Figs. S31 to S33, supporting that the dielectric breakdown strength and energy storage properties of the sandwich film **S-20** were well retained after 5,000 consecutive cyclic bending tests. Additionally, the dielectric spectra and breakdown strength of the sandwich film did

not exhibit any significant changes after mechanical fatigue tests with different curvatures over five consecutive days. (Fig. S34). These results verify that the hierarchical hybrid dielectric film exhibits desirable operational reliability under electrical and mechanical stresses, satisfying an important prerequisite for practical capacitor application of these soft PVTC polymers.

3. Conclusion

We have presented a facile approach to incorporating COF nanoparticles into composite thin films of the PVTC polymer, resulting in all-organic, self-standing sandwich films with significantly improved dielectric strength and energy storage capacity compared to the native PVTC polymer. In contrast to conventional COF synthesis which typically produces bulk polycrystalline powders, an *in situ* synthetic protocol was adapted to generate uniform, spherical COF nanoparticles within minutes at room temperature, allowing the layer-by-layer fabrication of sandwich films with COF embedded in the middle layer and PVTC as both the top and bottom layers. Importantly, this synthetic protocol is compatible with the co-introduction of PVTC additives into the COF middle layer, granting the fine-tuning of COF-PVTC interfaces and compositions to achieve optimal electromechanical stability for high electric field operations. Significantly improved dielectric breakdown strength and mechanical modulus have been established in the composition-optimized thin films, leading to greatly enhanced discharged energy density that is about three-time as high as that of the pure PVTC film. Moreover, the substantially reduced leakage current and remnant polarization secure high energy efficiency (e.g., 80.7% at 700 MV m^{-1}) of the resultant sandwich film. Additional mechanistic insights into performance enhancement are gained from control experiments and theoretical modeling. The comparison of the sandwich films against those containing randomly dispersed COF nanoparticles highlighted the importance of hierarchical structures in suppressing the growth of dielectric breakdown channels, as further elucidated by finite element simulations and statistical validations. Through the demonstration of COF-reinforced dielectric polymeric nanocomposites for the first time, this work underscores the potential of leveraging the functionality of COFs for innovative designs of high-performing flexible dielectric materials. We anticipate that by utilizing program-controlled processing methods under comparable

conditions, larger-area composite films beyond the lab scale demonstrated here can be readily fabricated.

Declaration of Competing Interest

The authors declare that they have no known competing financial interests or personal relationships that could have appeared to influence the work reported in this paper.

Acknowledgements

This work was funded by the U.S. Department of Energy, Office of Science, Office of Basic Energy Sciences, Materials Sciences and Engineering Division under Contract No. DE-AC02-05CH11231 within the Inorganic/Organic Nanocomposites Program (KC3104). The work was carried out as a user project at the Molecular Foundry, a user facility supported by the Office of Science, Office of Basic Energy Sciences, of the U.S. Department of Energy under Contract No. DE-AC02-05CH11231. The authors thank Dr. Lin-Wang Wang and Dr. Zhigang Song for discussions on dielectric breakdown simulation, Dr. Jian Zhang, Dr. Sizhuo Yang, Dr. Yi-Hsien Lu and Dr. Miao Qi for discussions on experimental results, and Haijuan Zhang, Dr. Shihai Zhang, Liana M. Klivansky, Dr. Virginia Altoé, Dr. Eric A. Dailing and Dr. Steve W. Shelton for technical support.

Appendix A. Supporting information

Supplementary data associated with this article can be found in the online version at xxx.

References

[1] Q.K. Feng, S.L. Zhong, J.Y. Pei, Y. Zhao, D.L. Zhang, D.F. Liu, Y.X. Zhang, Z.M. Dang, Recent progress and future prospects on all-organic polymer dielectrics for energy storage capacitors, Chem. Rev. 122 (2022) 3820–3878. https://doi.org/10.1021/acs.chemrev.1c00793.

[2] B. Chu, X. Zhou, K. Ren, B. Neese, M. Lin, Q. Wang, F. Bauer, Q.M. Zhang, A dielectric polymer with high electric energy density and fast discharge speed, Science 313 (2006) 334–336. https://doi.org/10.1126/science.1127798.

[3] H. Luo, X. Zhou, C. Ellingford, Y. Zhang, S. Chen, K. Zhou, D. Zhang, C.R. Bowen, C. Wan, Interface design for high energy density polymer nanocomposites. Chem. Soc. Rev. 48 (2019) 4424–4465. https://doi.org/10.1039/C9CS00043G.

[4] Q. Li, L. Chen, M.R. Gadinski, S. Zhang, G. Zhang, H.U. Li, E. Iagodkine, A. Haque, L.Q. Chen, T.N. Jackson, Q. Wang, Flexible high-temperature dielectric materials from polymer nanocomposites, Nature 523 (2015) 576–579. https://doi.org/10.1038/nature14647.

[5] C. Yuan, Y. Zhou, Y. Zhu, J. Liang, S. Wang, S. Peng, Y. Li, S. Cheng, M. Yang, J. Hu, B. Zhang, R. Zeng, J. He, Q. Li, Polymer/molecular semiconductor all-organic composites for high-temperature dielectric energy storage, Nat. Commun. 11 (2020) 3919. https://doi.org/10.1038/s41467-020-17760-x.

[6] G. Wang, Z. Lu, Y. Li, L. Li, H. Ji, A. Feteira, D. Zhou, D. Wang, S. Zhang, I.M. Reaney, Electroceramics for high-energy density capacitors: current status and future perspectives, Chem. Rev. 121 (2021) 6124–6172. https://doi.org/10.1021/acs.chemrev.0c01264.

[7] H. Li, Y. Zhou, Y. Liu, L. Li, Y. Liu, Q. Wang, Dielectric polymers for high-temperature capacitive energy storage, Chem. Soc. Rev. 50 (2021) 6369–6400. https://doi.org/10.1039/D0CS00765J.

[8] H. Li, B.S. Chang, H. Kim, Z. Xie, A. Lainé, L. Ma, T. Xu, C. Yang, J. Kwon, S.W. Shelton, L.M. Klivansky, V. Altoé, B. Gao, A.M. Schwartzberg, Z. Peng, R.O. Ritchie, T. Xu, M. Salmeron, R. Ruiz, K.B. Sharpless, P. Wu, Y. Liu, High-performing polysulfate dielectrics for electrostatic energy storage under harsh conditions, Joule 7 (2023) 95–112. https://doi.org/10.1016/j.joule.2022.12.010.

[9] Z. Pan, L. Yao, J. Zhai, X. Yao, H. Chen, Interfacial coupling effect in organic/inorganic nanocomposites with high energy density, Adv. Mater. 30 (2018) 1705662. https://doi.org/10.1002/adma.201705662.

[10] Q. Li, F.Z. Yao, Y. Liu, G. Zhang, H. Wang, Q. Wang, High-temperature dielectric materials for electrical energy storage, Annu. Rev. Mater. Res. 48 (2018) 219–243. https://doi.org/10.1146/annurev-matsci-070317-124435.

[11] X. Wu, X. Chen, Q.M. Zhang, D.Q. Tan, Advanced dielectric polymers for energy storage, Energy Storage Mater. 44 (2022). 29-47. https://doi.org/10.1016/j.ensm.2021.10.010.

[12] J.W. Zha, M.S. Zheng, B.H. Fan, Z.M. Dang, Polymer-based dielectrics with high permittivity for electric energy storage: A review, Nano Energy 89 (2021) 106438. https://doi.org/10.1016/j.nanoen.2021.106438.

[13] M. Zhang, H. Yang, Y. Lin, Q. Yuan, H. Du, Significant increase in comprehensive energy storage performance of potassium sodium niobate-based ceramics via synergistic optimization strategy, Energy Storage Mater. 45 (2022) 861–868. https://doi.org/10.1016/j.ensm.2021.12.037

[14] Y. Lin, D. Li, M. Zhang, S. Zhan, Y. Yang, H. Yang, Q. Yuan, Excellent energy-storage properties achieved in $BaTiO_3$-based lead-free relaxor ferroelectric ceramics via domain engineering on the nanoscale, ACS Appl. Mater. Interfaces 11 (2019) 36824–36830. https://doi.org/10.1021/acsami.9b10819

[15] Prateek, V.K. Thakur, R.K. Gupta, Recent progress on ferroelectric polymer-based nanocomposites for high energy density capacitors: synthesis, dielectric properties, and future aspects, Chem. Rev. 116 (2016) 4260–4317. https://doi.org/10.1021/acs.chemrev.5b00495.

[16] M. Guo, J. Jiang, Z. Shen, Y.H. Lin, C.W. Nan, Y. Shen, High-energy-density ferroelectric polymer nanocomposites for capacitive energy storage: enhanced breakdown strength and improved discharge efficiency, Mater. Today 29 (2019) 49–67. https://doi.org/10.1016/j.mattod.2019.04.015.

[17] L. Zhu, Q. Wang, Novel ferroelectric polymers for high energy density and low loss dielectrics, Macromolecules 45 (2012) 2937–2954. https://doi.org/10.1021/ma2024057.

[18] N. Meng, X. Ren, G. Santagiuliana, L. Ventura, H. Zhang, J. Wu, H. Yan, M.J. Reece, E. Bilotti, Ultrahigh β-phase content poly (vinylidene fluoride) with relaxor-like ferroelectricity for high energy density capacitors, Nat. Commun. 10 (2019) 4535. https://doi.org/10.1038/s41467-019-12391-3.

[19] H. Li, F. Liu, B. Fan, D. Ai, Z. Peng, Q. Wang, Nanostructured ferroelectric-polymer composites for capacitive energy storage, Small Methods 2 (2018) 1700399. https://doi.org/10.1002/smtd.201700399

[20] C. Wang, X. Zhao, L. Ren, L. Yu, Y. Jin, W. Tan, W. Zheng, H. Li, L. Yang, R. Liao, Enhanced dielectric and energy storage properties of P(VDF-HFP) through elevating β-phase formation under unipolar nanosecond electric pulses, Appl. Phys. Lett. 122 (2023) 023903. https://doi.org/10.1063/5.0128998

[21] X. Qian, D. Han, L. Zheng, J. Chen, M. Tyagi, Q. Li, F. Du, S. Zheng, X. Huang, S. Zhang, J. Shi, H. Huang, X. Shi, J. Chen, H. Qin, J. Bernhlc, X. Chen, L.Q. Chen, L. Hong, Q.M. Zhang, High-entropy polymer produces a giant electrocaloric effect at low fields, Nature 600 (2021) 664–669. https://doi.org/10.1038/s41586-021-04189-5.

[22] X. Chen, H. Qin, X. Qian, W. Zhu, B. Li, B. Zhang, Q.M. Zhang, Relaxor ferroelectric polymer exhibits ultrahigh electromechanical coupling at low electric field, Science, 375 (2022) 1418-1422. https://doi.org/10.1126/science.abn0936.

[23] F. Xia, Z.Y. Cheng, H.S. Xu, H.F. Li, Q.M. Zhang, G.J. Kavarnos, R.Y. Ting, G. Abdul-Sadek, K.D. Belfield, High electromechanical responses in a poly (vinylidene fluoride–trifluoroethylene–chlorofluoroethylene) terpolymer, Adv. Mater. 14 (2002) 1574–1577. https://doi.org/10.1002/1521-4095(20021104)14:21<1574::AIDADMA1574>3.0.CO;2-%23.

[24] Z. Bao, C. Hou, Z. Shen, H. Sun, G. Zhang, Z. Luo, Z. Dai, C. Wang, X Chen, L. Li, Y. Yin, Y. Shen, X. Li, Negatively charged nanosheets significantly enhance the energy-storage capability of polymer-based nanocomposites, Adv. Mater. (2020) 32 1907227. https://doi.org/10.1002/adma.201907227.

[25] N. Zebouchi, M. Bendaoud, R. Essolbi, D. Malec, B. Ai, H. Giam, Electrical breakdown theories applied to polyethylene terephthalate films under the combined effects of pressure and temperature, J. Appl. Phys. 79 (1996) 2497. https://doi.org/10.1063/1.361178.

[26] J. Claude, Y. Lu, K. Li, Q. Wang, Electrical storage in poly (vinylidene fluoride) based ferroelectric polymers: correlating polymer structure to electrical breakdown strength, Chem. Mater. 20 (2008) 2078–2080. https://doi.org/10.1021/cm800160r.
[27] Q. Li, G. Zhang, F. Liu, K. Han, M.R. Gadinski, C. Xiong, Q. Wang, Solution-processed ferroelectric terpolymer nanocomposites with high breakdown strength and energy density utilizing boron nitride nanosheet, Energy Environ. Sci. 8 (2015) 922–931. https://doi.org/10.1039/C4EE02962C.
[28] F. Liu, Q. Li, Z. Li, L. Dong, C. Xiong, Q. Wang, Ternary PVDF-based terpolymer nanocomposites with enhanced energy density and high power density, Compos. A: Appl. Sci. Manuf. 109 (2018) 597–603. https://doi.org/10.1016/j.compositesa.2018.03.019.
[29] Y. Li, Y. Zhou, Y. Zhu, S. Cheng, C. Yuan, J. Hu, J. He, Q. Li, Polymer nanocomposites with high energy density and improved charge–discharge efficiency utilizing hierarchically-structured nanofillers, J. Mater. Chem. A 8 (2020) 6576–6585. https://doi.org/10.1039/D0TA01380C.
[30] J. Chen, Z. Shen, Q. Kang, X. Qian, S. Li, P. Jiang, X. Huang, Chemical adsorption on 2D dielectric nanosheets for matrix free nanocomposites with ultrahigh electrical energy storage, Sci. Bull. 67 (2022) 609–618. https://doi.org/10.1016/j.scib.2021.10.011.
[31] Y. Shang, Y. Feng, C. Zhang, T. Zhang, Q. Lei, Q. Chi, Double gradient composite dielectric with high energy density and efficiency, J. Mater. Chem. A 10 (2022) 15183–15195. https://doi.org/10.1039/D2TA02279F.
[32] J. Wang, Y. Xie, J. Liu, Z. Zhang, Y. Zhang, Towards high efficient nanodielectrics from linear ferroelectric P (VDF-TrFE-CTFE)-g-PMMA matrix and exfoliated mica nanosheets, Appl. Surf. Sci. 469 (2019) 437–445. https://doi.org/10.1016/j.apsusc.2018.11.073.
[33] Y. Zhu, P. Jiang, X. Huang, Poly (vinylidene fluoride) terpolymer and poly (methyl methacrylate) composite films with superior energy storage performance for electrostatic capacitor application, Compos. Sci. Technol. 179 (2019) 115–124. https://doi.org/10.1016/j.compscitech.2019.04.035.
[34] X. Zhang, Y. Shen, Z. Shen, J. Jiang, L.Q. Chen, C.W. Nan, Achieving high energy density in PVDF-based polymer blends: suppression of early polarization saturation and enhancement of breakdown strength, ACS Appl. Mater. Interfaces 8 (2016) 27236–27242. https://doi.org/10.1021/acsami.6b10016.
[35] P. Shao, J. Li, F. Chen, L. Ma, Q. Li, M. Zhang, J. Zhou, A. Yin, X. Feng, B. Wang, Flexible films of covalent organic frameworks with ultralow dielectric constants under high humidity, Angew. Chem. Int. Ed. 57 (2018) 16501–16505. https://doi.org/10.1002/anie.201811250.
[36] A.M. Evans, A. Giri, V.K. Sangwan, S.N. Xun, M. Bartnof, C.G. Torres-Castanedo, H.B. Balch, M.S. Rahn, N.P. Bradshaw, E. Vitaku, D.W. Burke, H. Li, M.J. Bedzyk, F. Wang, J.L. Bredas, J.A. Malen, A. J.H. McGaughey, M.C. Hersam, W.R. Dichtel, P.E. Hopkins, Thermally conductive ultra-low-k dielectric layers based on two-dimensional covalent organic frameworks, Nat. Mater. 20 (2021) 1142–1148. https://doi.org/10.1038/s41563-021-00934-3.
[37] C. Wiraja, Y. Zhao, Toward miniaturizing microelectronics using covalent organic framework dielectric, Matter 4 (2021) 1760–1762. https://doi.org/10.1016/j.matt.2021.04.021.
[38] A.P. Côté, A.I. Benin, N.W. Ockwig, M.O'Keeffe, A.J. Matzger, O.M. Yaghi, Porous, crystalline, covalent organic frameworks, Science 310 (2005) 1166–1170. https://doi.org/10.1126/science.1120411.

[39] K.T. Tan, S. Ghosh, Z. Wang, F. Wen, D. Rodríguez-San-Miguel, J. Feng, N. Huang, W. Wang, F. Zamora, X. Feng, A. Thomas, D. Jiang, Covalent organic frameworks, Nat. Rev. Dis. Primers 3 (2023) 1. https://doi.org/10.1038/s43586-022-00181-z.
[40] Q. Fang, C. Sui, C. Wang, T. Zhai, J. Zhang, J. Liang, H. Guo, E. Sandoz-Rosado, J. Lou, Strong and flaw-insensitive two-dimensional covalent organic frameworks, Matter 4 (2021) 1017–1028. https://doi.org/10.1016/j.matt.2021.01.001.
[41] R. Freund, O. Zaremba, G. Arnauts, R. Ameloot, G. Skorupskii, M. Dincă, A. Bavykina, J. Gascon, A. Ejsmont, J. Goscianska, M. Kalmutzki, U. Lächelt, E. Ploetz, C.S. Diercks, S. Wuttke, The current status of MOF and COF applications, Angew. Chem. Int. Ed. 60 (2021) 23975–24001. https://doi.org/10.1002/anie.202106259.
[42] X. Li, S. Cai, B. Sun, C. Yang, J. Zhang, Y. Liu, Chemically robust covalent organic frameworks: progress and perspective, Matter 3 (2020) 1507–1540. https://doi.org/10.1016/j.matt.2020.09.007.
[43] Y. Liu, W. Zhou, W. L. Teo, K. Wang, L. Zhang, Y. Zeng, Y. Zhao, Covalent-organic-framework-based composite materials, Chem 6 (2020) 3172–3202. https://doi.org/10.1016/j.chempr.2020.08.021.
[44] H.S. Sasmal, A. Kumar Mahato, P. Majumder, R. Banerjee, Landscaping covalent organic framework nanomorphologies, J. Am. Chem. Soc. 144 (2022) 11482–11498. https://doi.org/10.1021/jacs.2c02301.
[45] W. Ma, Q. Zheng, Y. He, G. Li, W. Guo, Z. Lin, L. Zhang, Size-controllable synthesis of uniform spherical covalent organic frameworks at room temperature for highly efficient and selective enrichment of hydrophobic peptides, J. Am. Chem. Soc. 141 (2019) 18271–18277. https://doi.org/10.1021/jacs.9b09189.
[46] X. Zhang, J. Jiang, Z. Shen, Z. Dan, M. Li, Y.H. Lin, C.W. Nan, L.Q. Chen, Y. Shen, Polymer nanocomposites with ultrahigh energy density and high discharge efficiency by modulating their nanostructures in three dimensions, Adv. Mater. 30 (2018) 1707269. https://doi.org/10.1002/adma.201707269.
[47] Y. Niu, J. Dong, Y. He, X. Xu, S. Li, K. Wu, Q. Wang, H. Wang, Significantly enhancing the discharge efficiency of sandwich-structured polymer dielectrics at elevated temperature by building carrier blocking interface, Nano Energy, 97 (2022) 107215. https://doi.org/10.1016/j.nanoen.2022.107215.
[48] J.W. Zha, Y. Tian, M.S. Zheng, B. Wan, X. Yang, G. Chen, High-temperature energy storage polyimide dielectric materials: polymer multiple-structure design, Mater. Today Energy 31 (2023) 101217. https://doi.org/10.1016/j.mtener.2022.101217.
[49] T. Ju, X. Chen, D. Langhe, M. Ponting, E. Baer, L. Zhu, Enhancing breakdown strength and lifetime of multilayer dielectric films by using high temperature polycarbonate skin layers, Energy Storage Mater. 45 (2022) 494–503. https://doi.org/10.1016/j.ensm.2021.12.009.
[50] F. Liu, Q. Li, J. Cui, Z. Li, G. Yang, Y. Liu, L. Dong, C. Xiong, H. Wang, Q. Wang, High-energy-density dielectric polymer nanocomposites with trilayered architecture, Adv. Funct. Mater. 27 (2017) 1606292. https://doi.org/10.1002/adfm.201606292.
[51] Y. Wang, J. Cui, Q. Yuan, Y. Niu, Y. Bai, H. Wang, Significantly enhanced breakdown strength and energy density in sandwich-structured barium titanate/poly (vinylidene fluoride) nanocomposites, Adv. Mater. 27 (2015) 6658–6663. https://doi.org/10.1002/adma.201503186.
[52] D. Zhao, Q. Cai, X. Zhu, W. Xu, Q. Zhou, S. Niu, Z. Jiang, Y. Zhang. Multilayer dielectric nanocomposites with cross-linked dielectric transition interlayers for high-temperature

applications, ACS Appl. Mater. Interfaces 14 (2022) 42531–42540. https://doi.org/10.1021/acsami.2c12590.
[53] Z. Pan, B. Liu, J. Zhai, L. Yao, K. Yang, B. Shen, $NaNbO_3$ two-dimensional platelets induced highly energy storage density in trilayered architecture composites, Nano Energy 40 (2017) 587–595. https://doi.org/10.1016/j.nanoen.2017.09.004.
[54] Y. Lin, Y. Zhang, S. Zhan, C. Sun, G. Hu, H. Yang, Q. Yuan, Synergistically ultrahigh energy storage density and efficiency in designed sandwich-structured poly (vinylidene fluoride)-based flexible composite films induced by doping $Na_{0.5}Bi_{0.5}TiO_3$ whiskers, J. Mater. Chem. A 8 (2020) 23427–23435. https://doi.org/10.1039/D0TA07937E
[55] H. Li, T. Yang, Y. Zhou, D. Ai, B. Yao, Y. Liu, L. Li, L.Q. Chen, Q. Wang, Enabling high-energy-density high-efficiency ferroelectric polymer nanocomposites with rationally designed nanofillers, Adv. Funct. Mater. 31 (2021) 2006739. https://doi.org/10.1002/adfm.202006739.
[56] Y. Zhu, Y. Zhu, X. Huang, J. Chen, Q. Li, J. He, P. Jiang, High energy density polymer dielectrics interlayered by assembled boron nitride nanosheets, Adv. Energy Mater. 9 (2019) 1901826. https://doi.org/10.1002/aenm.201901826.
[57] T. Wang, R. Peng, W. Peng, G. Dong, C. Zhou, S. Yang, Z. Zhou, M. Liu, 2–2 type PVDF-based composites interlayered by epitaxial (111)-oriented BTO films for high energy storage density, Adv. Funct. Mater. 32 (2021) 2108496. https://doi.org/10.1002/adfm.202108496.
[58] T. Zhang, L. Yang, C. Zhang, Y. Feng, J. Wang, Z. Shen, Q. Chen, Q. Lei, Q. Chi, Polymer dielectric films exhibiting superior high-temperature capacitive performance by utilizing an inorganic insulation interlayer, Mater. Horiz. 9 (2022) 1273–1282. https://doi.org/10.1039/D1MH01918J.
[59] Y. Wang, L. Wang, Q. Yuan, Y. Niu, J. Chen, Q. Wang, H. Wang, Ultrahigh electric displacement and energy density in gradient layer-structured $BaTiO_3$/PVDF nanocomposites with an interfacial barrier effect, J. Mater. Chem. A 5 (2022) 10849–10855. https://doi.org/10.1039/C7TA01522D.
[60] M. Yuan, B. Li, S. Zhang, R. Rajagopalan, M.T. Lanagan, High-field dielectric properties of oriented poly (vinylidene fluoride-*co*-hexafluoropropylene): structure–dielectric property relationship and implications for energy storage application, ACS Appl. Polym. Mater. 2 (2020) 1356–1368. https://doi.org/10.1021/acsapm.9b01224
[61] A.K. Jonscher, Dielectric relaxation in solids, J. Phys. D: Appl. Phys. 32 (1999) R57–R70. https://doi.org/10.1088/0022-3727/32/14/201
[62] T. Zhu, H. Zhao, N. Zhang, C. Zhang, L. Yin, Z.M. Dang, J. Bai, Ultrahigh energy storage density in poly (vinylidene fluoride)-based composite dielectrics via constructing the electric potential well, Adv. Energy Mater. 13 (2023) 2203587. https://doi.org/10.1002/aenm.202203587.
[63] J. Liu, L. Ji, J. Yu, S. Ding, S. Luo, B. Chu, J. Xu, R. Sun, S. Yu, Enhanced breakdown strength and electrostatic energy density of polymer nanocomposite films realized by heterostructure ZnO-ZnS nanoparticles, Chem. Eng. J. 456 (2023) 140950. https://doi.org/10.1016/j.cej.2022.140950.
[64] D. Ai, H. Li, Y. Zhou, L. Ren, Z. Han, B. Yao, W. Zhou, L. Zhao, J. Xu, Q. Wang, Tuning nanofillers in in situ prepared polyimide nanocomposites for high-temperature capacitive energy storage, Adv. Energy Mater. 10 (2020) 1903881. https://doi.org/10.1002/aenm.201903881.

[65] Y. Hao, X. Wang, K. Bi, J. Zhang, Y. Huang, L. Wu, P. Zhao, M. Lei, L. Li, Significantly enhanced energy storage performance promoted by ultimate sized ferroelectric $BaTiO_3$ fillers in nanocomposite films, Nano Energy, 31 (2017) 49-56. https://doi.org/10.1016/j.nanoen.2016.11.008

[66] J. Jiang, Z. Shen, J. Qian, Z. Dan, M. Guo, Y.H. Lin, C.W. Nan, L.Q. Chen, Y. Shen, Ultrahigh discharge efficiency in multilayered polymer nanocomposites of high energy density, Energy Storage Mater. 18 (2019) 213–221. https://doi.org/10.1016/j.ensm.2018.09.013.

[67] C. Wang, G. He, S. Chen, D. Zhai, H. Luo, D. Zhang. Enhanced performance of all-organic sandwich structured dielectrics with linear dielectric and ferroelectric polymers, J. Mater. Chem. A 9 (2021) 8674–8684. https://doi.org/10.1039/D1TA00974E.

[68] Y. Zhang, C. Zhang, Y. Feng, T. Zhang, Q. Chen, Q. Chi, L. Liu, X. Wang, Q. Lei, Energy storage enhancement of P(VDF-TrFE-CFE)-based composites with double-shell structured BZCT nanofibers of parallel and orthogonal configurations, Nano Energy 66 (2019) 1041195. https://doi.org/10.1016/j.nanoen.2019.104195.

[69] Y. Shang, Y. Feng, C. Li, C. Zhang, T. Zhang, Y. Zhang, Y. Zhang, C. Song, Q. Chi, Energy storage properties of P(VDF-TrFE-CTFE)-based composite dielectrics with uniform and gradient-doped boron nitride nanosheets, IET Nanodielectr. 5 (2022) 50–61. https://doi.org/10.1049/nde2.12024.

[70] L. Wang, H. Luo, X. Zhou, X. Yuan, K. Zhou, D. Zhang, Sandwich-structured all-organic composites with high breakdown strength and high dielectric constant for film capacitor, Compos. A: Appl. Sci. Manuf. 117 (2019) 369–376. https://doi.org/10.1016/j.compositesa.2018.12.007.

[71] B. Li, H. Zhang, S. Zhang, Techniques for capacitor dielectrics characterization in: Q. Li (Eds.), Advanced Dielectric Materials for Electrostatic Capacitors, The Institution of Engineering and Technology, London, 2020, pp. 33–69.

[72] F. Guan, J. Wang, J. Pan, Q. Wang, L. Zhu, Effects of polymorphism and crystallite size on dipole reorientation in poly (vinylidene fluoride) and its random copolymers, Macromolecules 43 (2010) 6739-6748. https://doi.org/10.1021/ma101062j.

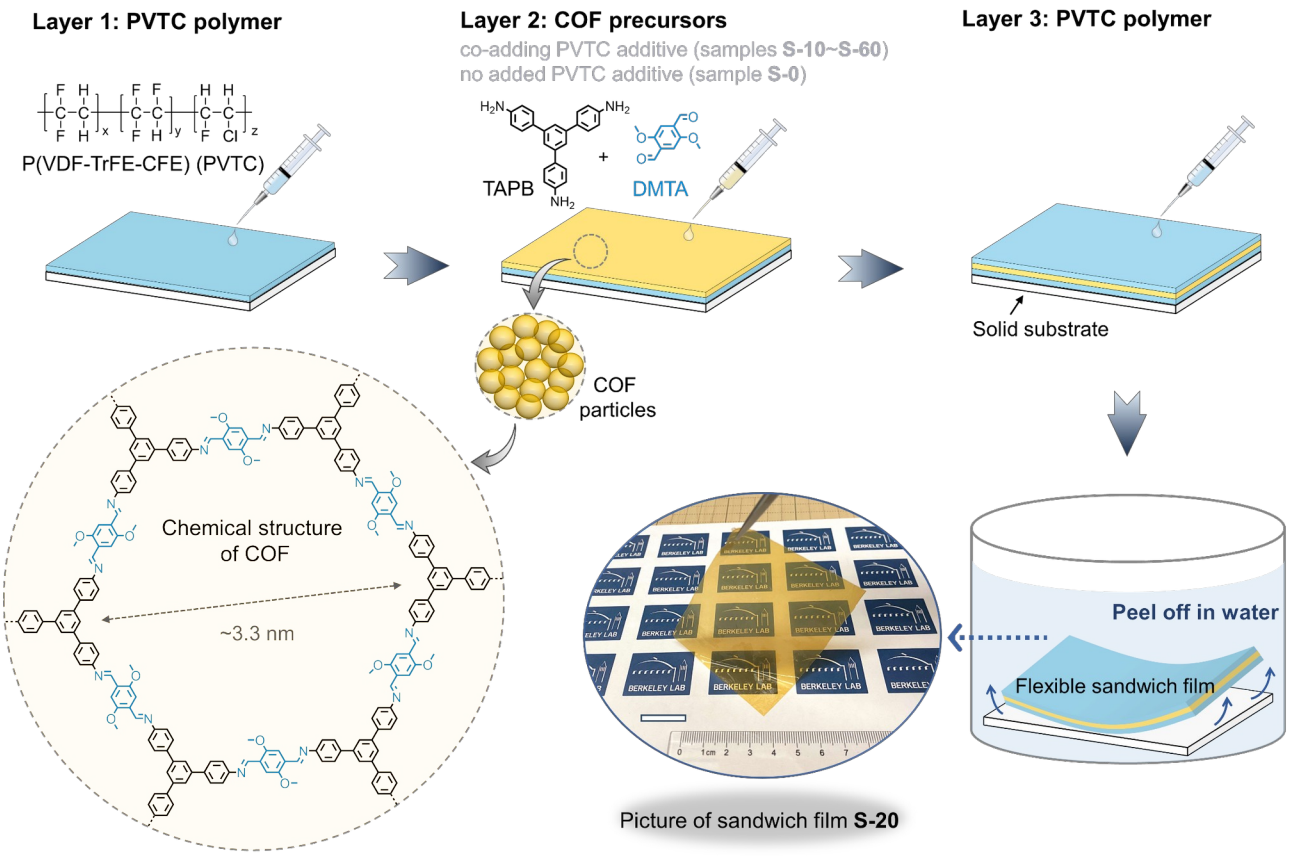

Scheme 1. The scheme of sandwich-structured film preparation using a layer-by-layer solution casting method, as well as the chemical structure of imine-linked COF and a picture of sandwich PVTC/COF composite film **S-20**. The scale bar in the embedded picture is 2 cm.

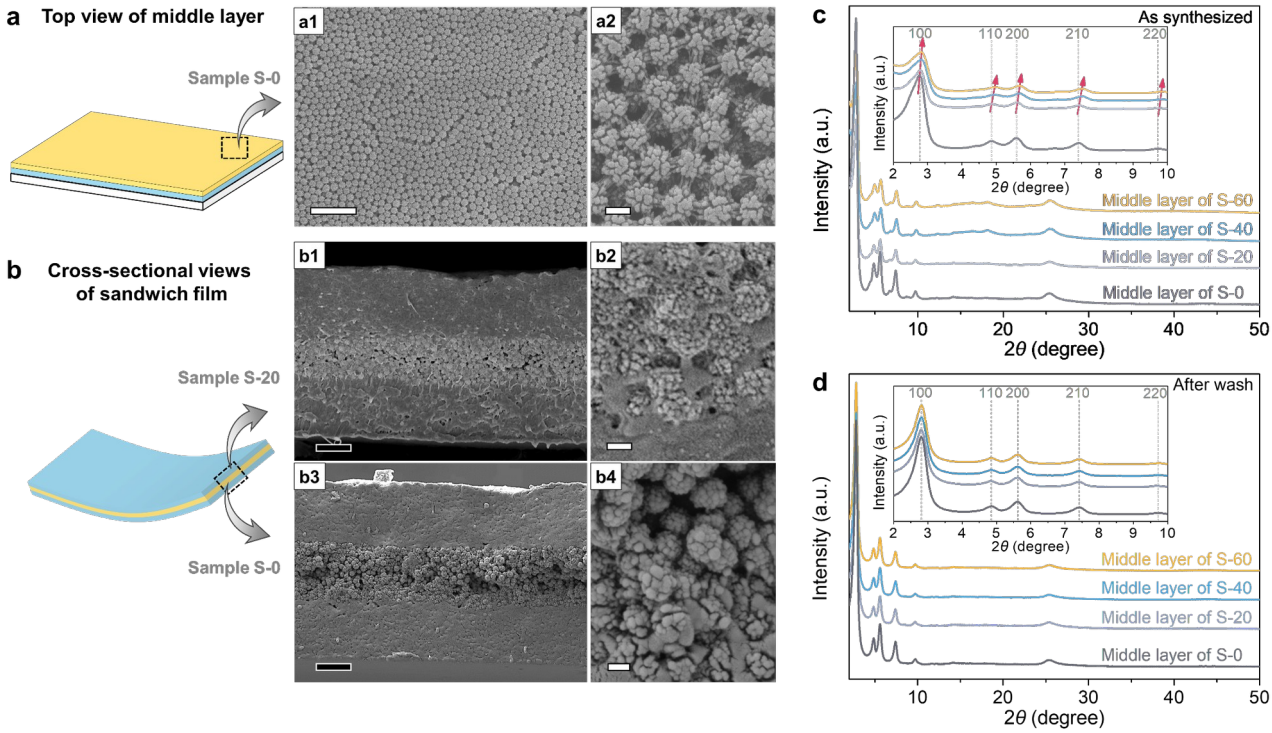

Fig. 1. **(a)** The scheme of the top view of layer 2, and the corresponding SEM images of COF nanospheres. **(b)** The scheme of cross-sectional views of the sandwich films, and the corresponding SEM images of *in situ* synthesized **S-20** and **S-0** film samples. XRD profiles of COF-containing middle layer (layer 2): **(c)** As-obtained materials without wash, and **(d)** materials after wash. The scale bars in (**a1**), (**b1**) and (**b3**) are 2 μm; The scale bars in **(a2)**, **(b2)** and **(b4)** are 200 nm.

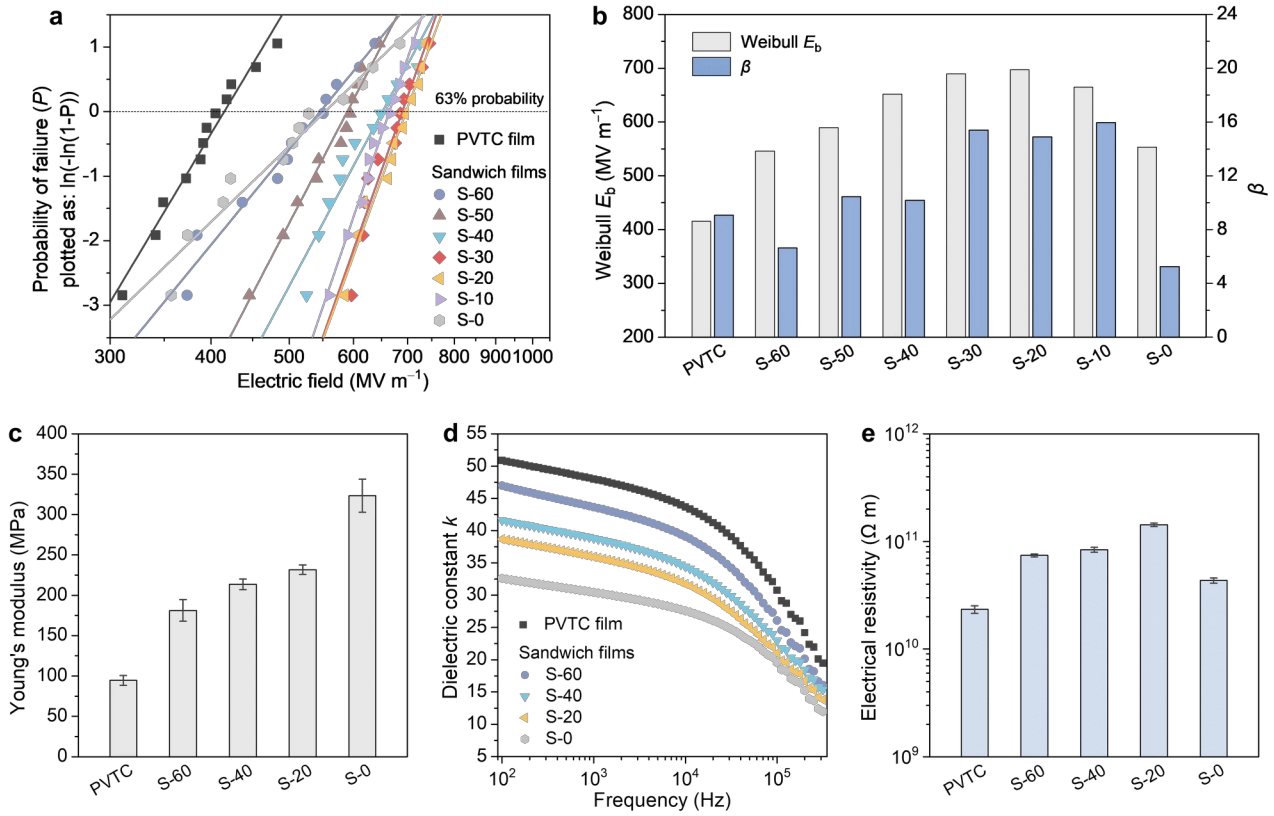

Fig. 2. **(a)** Weibull plots of native PVTC and *in situ* synthesized sandwich PVTC/COF films. **(b)** Weibull E_b and β values **(c)** Young's modulus (Y), **(d)** Frequency-dependent spectra of dielectric constant (k) and **(e)** Electrical resistivity of native PVTC and *in situ* synthesized sandwich PVTC/COF films. Error bars show standard deviations obtained from at least three measurements using different samples.

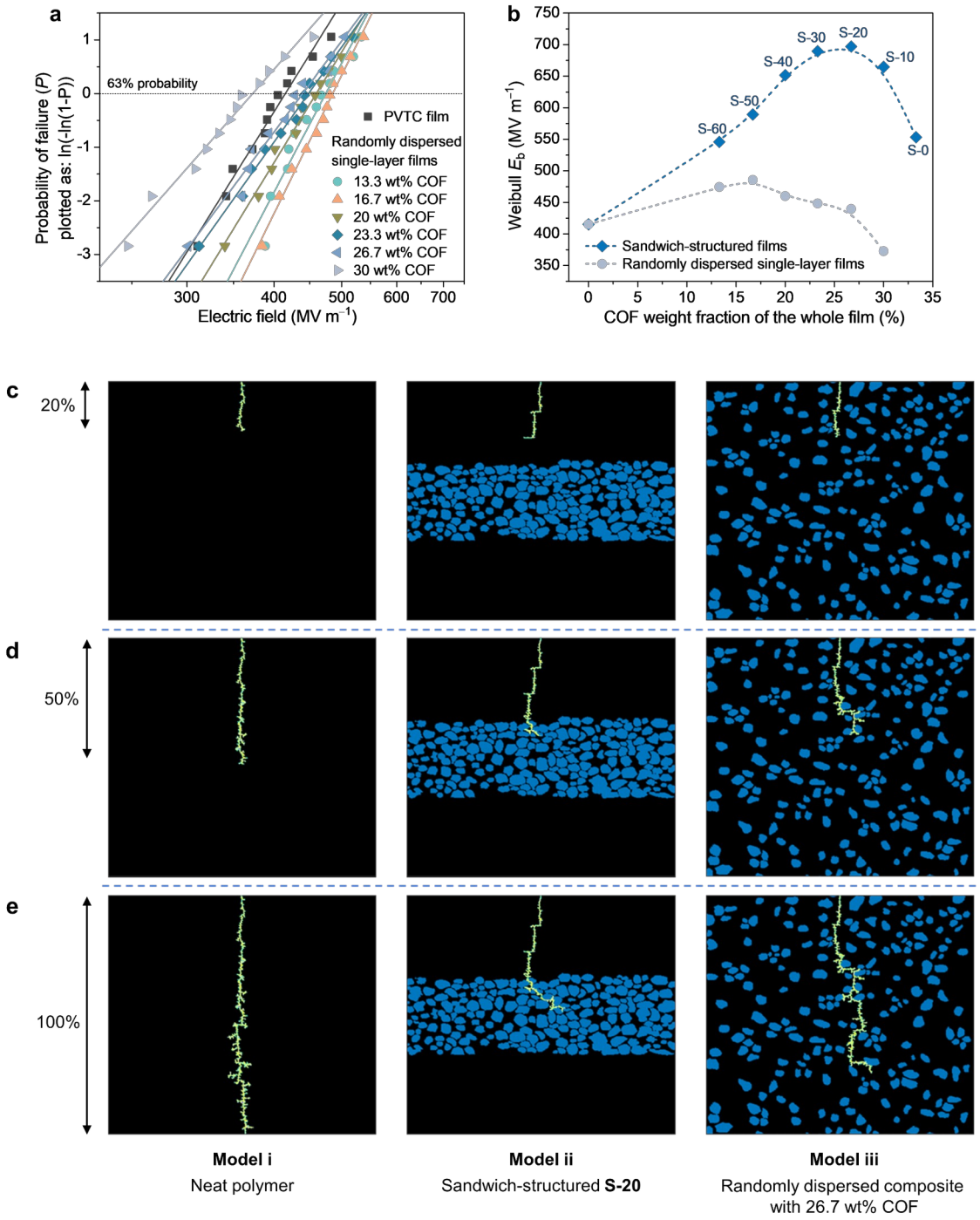

Fig. 3. **(a)** Weibull plots of native PVTC film and randomly dispersed single-layer PVTC/COF films with various COF loading ratios. **(b)** Weibull E_b of sandwich-structured and randomly dispersed single-layer films as a function of COF weight fraction. Finite element simulations of breakdown channels based on **Model i**, **Model ii** and **Model iii** at different stages: **(c)** 20%, **(d)** 50% and **(e)** 100% propagation ratios of breakdown channels, taking **Model i** as a reference. The applied electric field for simulation is 400 MV m^{-1}. The model size for all simulations is 9 μm × 9 μm.

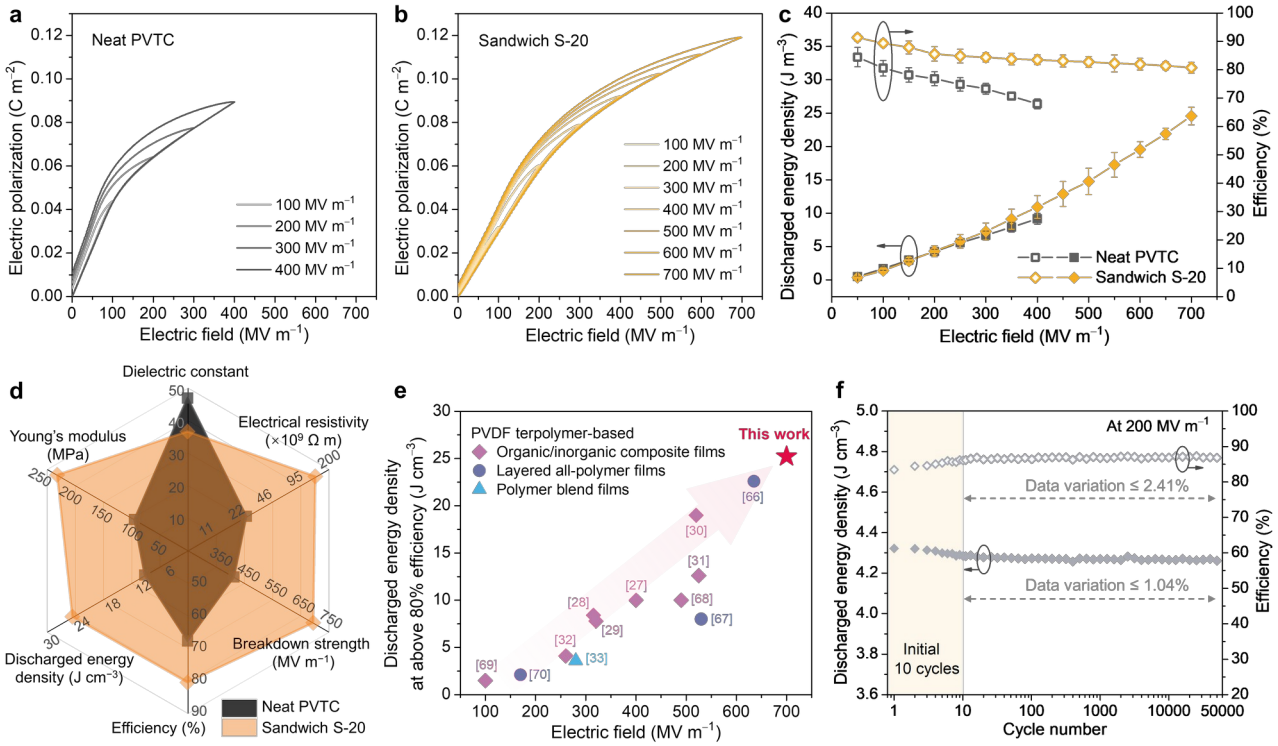

Fig. 4. *P-E* loops of **(a)** native PVTC film and **(b)** *in situ* synthesized sandwich PVTC/COF (**S-20**) film. **(c)** Discharged energy density (U_d) and charge-discharge efficiency (η) of native PVTC and *in situ* synthesized sandwich PVTC/COF (**S-20**) films as a function of electric field. **(d)** Radar chart: comparison of mechanical, electrical and energy storage parameters of native PVTC and *in situ* synthesized sandwich PVTC/COF (**S-20**) films. Electrical resistivity is presented using a logarithmic coordinate, other properties are presented using linear coordinates. **(e)** Performance comparison of the discharged energy density (U_d) values at above 80% efficiency and their corresponding applied electric fields among **S-20** film and other reported PVDF terpolymer-based dielectric materials, including organic/inorganic composite films, layered all-polymer films and polymer blend films.[27-33, 66-70] **(f)** Charging/discharging cyclic test results of sandwich **S-20** film measured under 200 MV m^{-1}. Error bars show standard deviations obtained from at least three measurements using different samples.